Langmuir
Article
pubs.acs.org/Langmuir

Effect of TiO_2 Nanoparticles on Self-Assembly Behaviors and Optical and Photovoltaic Properties of the P3HT-*b*-P2VP Block Copolymer

Wei-Che Yen,[†] Yi-Huan Lee,[†] Jhih-Fong Lin,[‡] Chi-An Dai,[†,§] U-Ser Jeng,[∥] and Wei-Fang Su*[,†,‡]

[†]*Institute of Polymer Science and Engineering,* [‡]*Department of Material Science and Engineering, and* [§]*Department of Chemical Engineering, National Taiwan University, Taipei, Taiwan, and* [∥]*National Synchrotron Radiation Research Center, Hsinchu, Taiwan*

Received October 3, 2010. Revised Manuscript Received November 6, 2010

An ordered nanostructure can be created from the hybrid materials of self-assembly poly(3-hexyl thiophene-*b*-2-vinyl pyridine) and nicotinic acid-modified titanium dioxide nanoparticles (P3HT-*b*-P2VP/TiO_2). TEM and XRD analyses reveal that the TiO_2 nanoparticles (NPs) are preferentially confined in the P2VP domain of P3HT-*b*-P2VP whereas TiO_2 NPs interact with either pure P3HT or a blend of P3HT and P2VP to produce microsized phase segregation. The morphologies of lamellar and cylindrical structures are disturbed when the loading of TiO_2 NPs is 40 wt % or higher. Cylindrical P3HT-*b*-P2VP/TiO_2 exhibits a small blue shift in absorption and photoluminescence spectra with increasing TiO_2 loading as compared to P3HT/TiO_2. The NPs cause a slightly misaligned P3HT domain in the copolymer. Furthermore, the PL quenching of P3HT-*b*-P2VP/TiO_2 becomes very large as a result of efficient charge separation in the ordered nanodomain at 16 nm. Solar cells fabricated from self-assembly P3HT-*b*-P2VP/TiO_2 hybrid materials exhibit a >30 fold improvement in power conversion efficiency as compared to the corresponding 0.3P3HT-0.7P2VP/TiO_2 polymer blend hybrid. This study paves the way for the further development of high-efficiency polymer−inorganic nanoparticle hybrid solar cells using a self-assembled block copolymer.

Introduction

Block copolymers have attracted increasing amounts of interest because of their ability to self-organize into periodic nanodomains ranging from 5 to 50 nm,[1] which encompasses the dimensional requirements for the fabrication of future integrated circuits[2] and bulk heterojunction (BHJ) solar cells.[3] Self-assembled insulating coil−coil block copolymers are currently pursued to replace polymeric photoresist films beyond the 22 nm node.[4] The bulk heterojunction solar cells are fabricated from a blend of a conducting polymer (donor) and a semiconducting nanoparticle (acceptor) hybrid. The hybrid is capable of forming a bicontinuous phase with a domain size smaller than the exciton diffusion length of the conducting polymer (<20 nm).[5,6] A high-performance BHJ solar cell should have large interfaces for efficient charge separation and continuous phase separation for charge transport. Therefore, morphological control of the polymer−nanoparticle hybrid must be carefully considered with respect to its role in the BHJ structure. By using suitable molecular weights and compositions, the domain size of the separated phase in block copolymers can be easily controlled to within 20 nm. Therefore, solar cells fabricated from ordered hybrids based on a self-assembled block copolymer are expected to have an improved power conversion efficiency.[7]

Our previous work[8] indicates that the rod−coil block copolymer of P3HT-*b*-P2VP exhibited self-assembling spherical (wt $\%_{P3HT} = 14$), cylindrical (wt $\%_{P3HT} = 25$), lamellar (wt $\%_{P3HT} = 41$), and fibrillar (wt $\%_{P3HT} = 60$) morphologies when P3HT with a weight-average molecular weight of 7K Da was anionically copolymerized with the 2-VP monomer. We have observed the domain size of the separated phase ranging from 15 to 30 nm. Thus, our P3HT-*b*-P2VP copolymer is a good candidate material for meeting the required properties in bulk heterojunction solar cell fabrication.

The blending of nanoparticles with self-assembled insulating block copolymers has been extensively studied.[9−17] However, there have been few reports on the BHJs made from self-assembled conducting block copolymers containing nanoparticles for solar cell applications.[18] Hadziioannou et al.[19,20] and Fréchet et al.[21] used systems where C_{60} is attached to the insulating segment of the conducting−insulating block copolymer. Others have

*Corresponding author. Tel: 886-2-3366-4078. Fax: 886-2-3366-4078. E-mail: suwf@ntu.edu.tw.

(1) Bates, F. S.; Fredrickson, G. H. *Phys. Today* **1999**, *52*, 32.
(2) Kim, H. C.; Park, S. M.; Hinsberg, W. D. *Chem. Rev.* **2010**, *110*, 146.
(3) Heeger, A. J.; Yu, G.; Gao, J.; Hummelen, J. C.; Wudl, F. *Science* **1995**, *270*, 1789.
(4) Mack, C. A. *Future Fabr. Int.* **2007**, *23*, 65.
(5) Clarke, T. M.; Durrant, J. R. *Chem. Rev* **2010**, *110*, 6736.
(6) Saunders, B. R.; Turner, M. L. *Adv. Colloid Interface Sci.* **2008**, *138*, 1.
(7) Shah, M.; Ganesan, V. *Macromolecules* **2010**, *43*, 543.
(8) Dai, C. A.; Yen, W. C.; Lee, Y. H.; Ho, C. C.; Su, W. F. *J. Am. Chem. Soc.* **2007**, *129*, 11036.
(9) Lopes, W. A.; Jaeger, H. M. *Nature* **2001**, *414*, 735.
(10) Lin, Y.; Boker, A.; He, J. B.; Sill, K.; Xiang, H. Q.; Abetz, C.; Li, X. F.; Wang, J.; Emrick, T.; Long, S.; Wang, Q.; Balazs, A.; Russell, T. P. *Nature* **2005**, *434*, 55.
(11) Kim, B. J.; Chiu, J. J.; Yi, G.-R.; Pine, D. J.; Kramer, E. J. *Adv. Mater.* **2005**, *17*, 2618.
(12) Deshmukh, R. D.; Buxton, G. A.; Clarke, N.; Composto, R. J. *Macromolecules* **2007**, *40*, 6316.
(13) Chiu, J. J.; Kim, B. J.; Kramer, E. J.; Pine, D. J. *J. Am. Chem. Soc.* **2005**, *127*, 5036.
(14) Zou, S.; Hong, R.; Emrick, T.; Walker, G. C. *Langmuir* **2007**, *23*, 1612.
(15) Deshmukh, R. D.; Liu, Y.; Composto, R. J. *Nano Lett* **2007**, *7*, 3662.
(16) Zhang, Q-L; Gupta, S.; Emrick, T.; Russell, T. P. *J. Am. Chem. Soc.* **2006**, *128*, 3898.
(17) Bockstaller, M. R.; Mickiewicz, R. A.; Thomas, E. L. *Adv. Mater.* **2005**, *17*, 1331.
(18) Sary, N.; Richard, F.; Brochon, C.; Leclerc, N.; Lévêque, P.; Audinot, J. N.; Berson, S.; Heiser, T.; Hadziioannou, G..; Mezzenga, R. *Adv. Mater.* **2009**, *21*, 1.
(19) Stalmach, U.; de Boer, B.; Videlot, C.; van Hutten, P. F.; Hadziioannou, G. *J. Am. Chem. Soc.* **2000**, *122*, 5464.
(20) van der Veen, M. H.; de Boer, B.; Stalmach, U.; Van de Wetering, K.; Hadziioannou, G. *Macromolecules* **2004**, *37*, 3673.
(21) Sivula, K.; Ball, Z. T.; Watanabe, N.; Fréchet, J. M. J. *Adv. Mater.* **2006**, *18*, 206.

synthesized organic donor/acceptor block copolymers for solar cell applications.[22−24]

In this report, we study the changes in the morphological, optical, and photovoltaic properties of the self-assembled P3HT-*b*-P2VP block copolymer with varying numbers of TiO_2 NPs. TiO_2 NPs are modified with nicotinic acid to have good affinity for the P2VP segment. Through the interaction of the TiO_2 NP and P2VP domain, the TiO_2 NPs are preferentially located in the P2VP domain at high order.

Experimental Section

Materials. All reagents and chemicals were purchased from Aldrich Chemical Co. and used as received.

Synthesis and Modification of TiO_2 NPs. Anatase TiO_2 NPs in an acidic aqueous solution were synthesized by a sol−gel reaction.[25] Then, the TiO_2 NPs solution was concentrated into a gel-like state by rotary evaporation. TiO_2 NPs were modified by adding concentrated NPs to a nicotinic acid solution (10 g nicotinic acid dissolved in 200 mL of methanol). This solution was stirred overnight, resulting in modified NPs that were then separated from solution by concentration, centrifugation, and decantation of the solution. The excess ligand was removed by repeating the above process three times with methanol. Finally, a 5 wt % solution of nicotinic acid-modified TiO_2 NPs was prepared in a cosolvent of methanol/pyridine (5/1, v/v). FT-IR measurements were used to confirm the nicotinic acid that was chemically linked to the surfaces of TiO_2 NPs.

Preparation of P3HT-P2VP Block Copolymers. The P3HT-*b*-P2VP's, having different compositions, were synthesized by anionically polymerizing 2-vinylpyridine monomer with a macroinitiator of poly(3-hexyl thiophyl lithium) according to a previous publication.[8] A vinyl-end-terminated P3HT can be activated at the terminal double bond with *sec*-butyl lithium (*s*-BuLi) for subsequent anionic polymerization. The detailed synthesis and characterization of P3HT-*b*-P2VPs were discussed in our previous publication.[8] The copolymers used in this study had spherical (M_w = 58 410, wt $\%_{P3HT}$ = 14), cylindrical (M_w = 25 864, wt $\%_{P3HT}$ = 25), and lamellar (M_w = 20 213, wt $\%_{P3HT}$ = 41) structures. Pure P3HT that was used for comparison was synthesized using the McCullough method,[26] and the weight-average molecular weight was 10 000 (PDI = 1.17).

Sample Preparation and Characterization of the Bulk Heterojunction. Polymers (50 mg of P3HT, the 0.3P3HT-0.7P2VP blend, or cylindrical P3HT-*b*-P2VP) were first dissolved in 2 mL of tetrahydrofuran (THF), followed by adding different amounts of TiO_2 NP solution to obtain the hybrid solution. For TEM, XRD, and SAXS measurements, bulk samples were prepared by slowly evaporating the hybrid solutions for 3 days at room temperature. The bulk samples were then microtomed, followed by floating the cut film on a copper grid coated with carbon for TEM observation. For SAXS experiments, a 1 mm thick washer was filled with a bulk sample and then placed in a vacuum oven for annealing at 135 °C for 2 days. For the study of UV−vis and PL spectra, thin films with different compositions were coated onto quartz via spin coating at 1000 rpm. A pellet of modified TiO_2 dry powder was used for FT-IR measurements.

The size of TiO_2 NPs and the morphologies of hybrids of polymers and NPs were evaluated by transmission electron microscopy (TEM, a JEOL 1230 microscope). The chemical structure of nicotinic acid-modified TiO_2 NPs was investigated

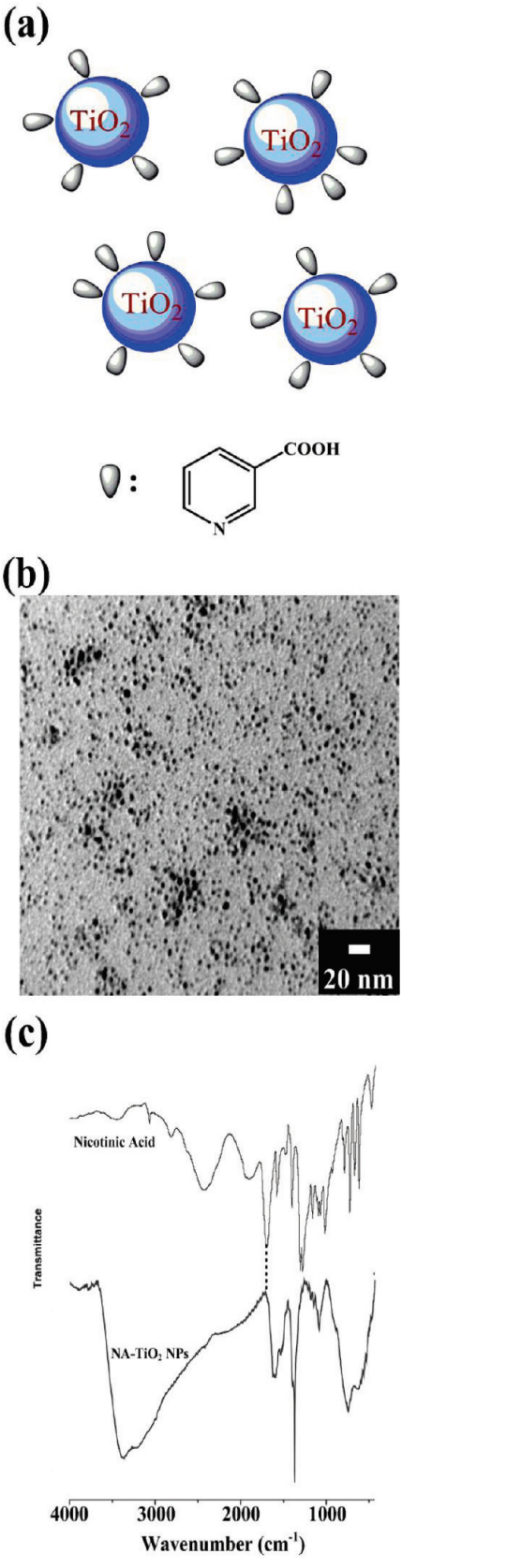

Figure 1. (a) Schematic representation of nicotinic acid-modified TiO_2 NPs, (b) their TEM image, and (c) IR spectra of nicotinic acid and NA-TiO_2 NPs.

(22) Lindner, S. M.; Huttner, S.; Chiche, A.; Thelakkat, M.; Krausch, G. *Angew. Chem., Int. Ed.* **2006**, *45*, 3364.
(23) Zhang, Q-L; Cirpan, A.; Russell, T. P.; Emrick, T. *Macromolecules* **2009**, *42*, 1079.
(24) Tao, Y.; McCulloch, B.; Kimc, S.; Segalman, R. A. *Soft Mater.* **2009**, *5*, 4219.
(25) Wang, P.; Zakeeruddin, S. M.; Comte, P.; Charvet, R.; Humphry-Baker, R.; Grätzel, M. *J. Phys. Chem. B* **2003**, *107*, 14336.
(26) Loewe, R. S.; Khersonsky, S. M.; MCcullough, R. D. *Adv. Mater.* **1999**, *11*, 250.

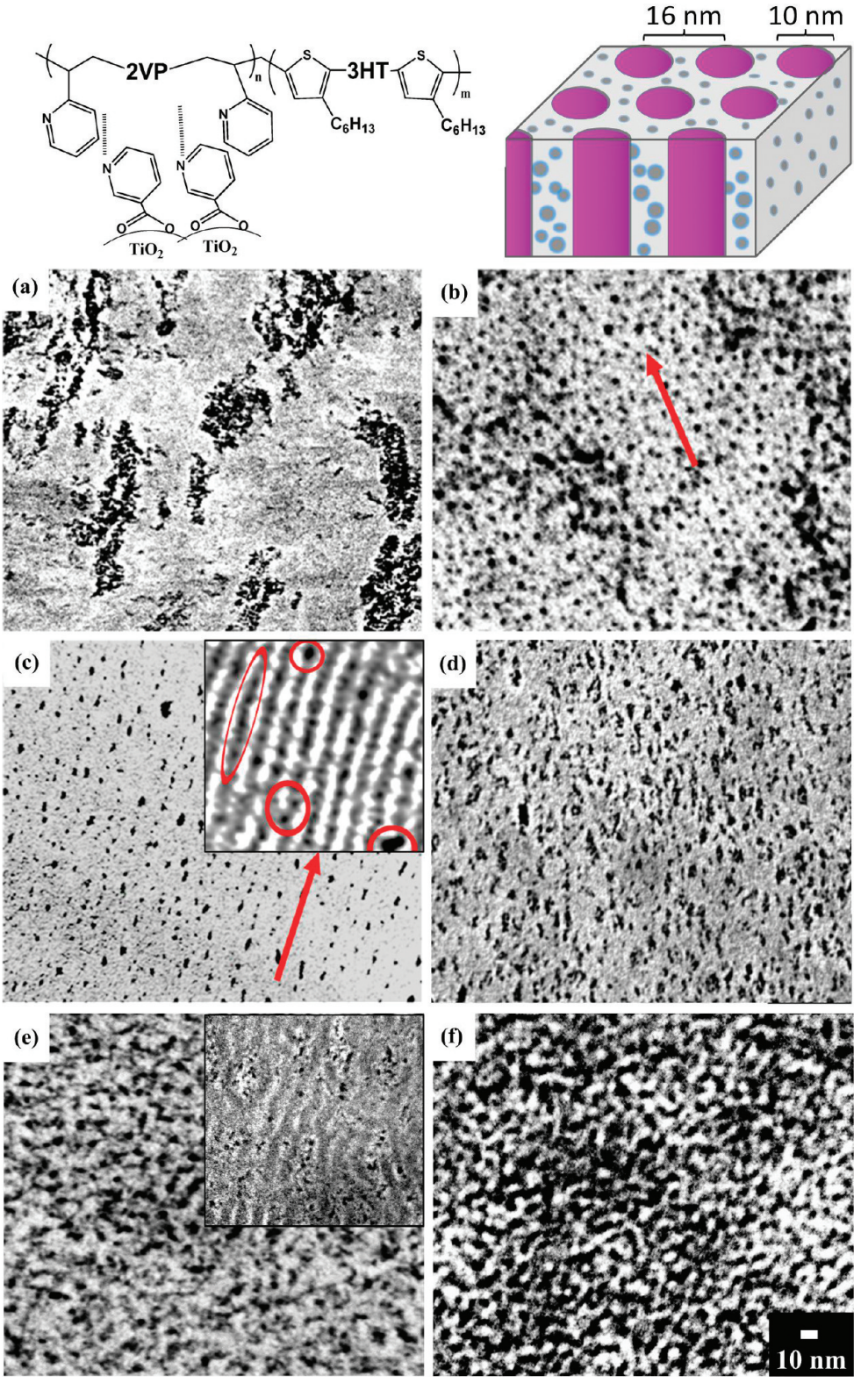

Figure 2. Schematic illustration of nicotinic acid-modified TiO_2 nanoparticles (NA-TiO_2 NPs) interacting and organizing with P3HT-*b*-P2VP. TEM images of the polymer hybrids/NA-TiO_2 NPs obtained by blending NA-TiO_2 NPs with (a) pure P3HT (40 wt % NPs), (b) a lamellar copolymer (10 wt % NPs), and (c) a cylindrical copolymer (10 wt % NPs, I_2-stained image in the inset). (d) Cylindrical copolymer (20 wt % NPs) and (e) cylindrical copolymer (40 wt % NPs, I_2-stained image in the inset). (f) Spherical copolymer (40 wt % NPs). The scale bar for all images is 10 nm.

by FT-IR (Perkin-Elmer Spectrum 100). Absorption spectra were recorded on a Perkin-Elmer Lambda 35 UV−vis spectrometer. The photoluminescence (PL) spectra were obtained by exciting the polymer samples at 450 nm, and the emission was measured with a Perkin-Elmer LS 55 luminescence spectrometer. The crystalline structure and long-range ordering of hybrids were observed by X-ray diffraction (XRD) and small-angle X-ray scattering (SAXS), respectively. These experiments were performed on

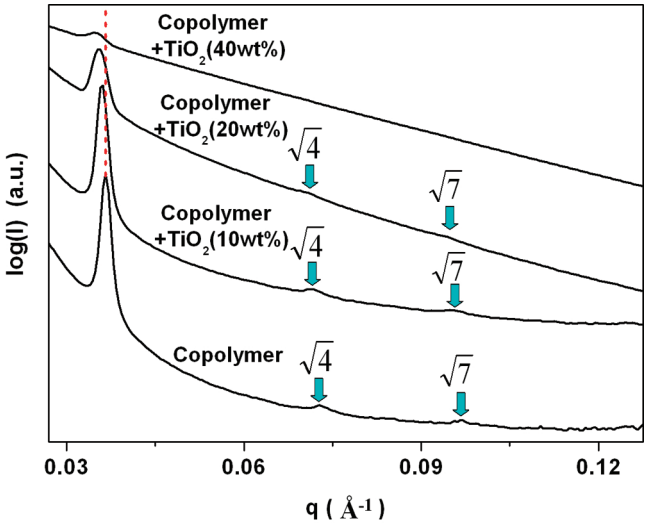

Figure 3. SAXS patterns of P3HT-*b*-P2VP incorporating different amounts of TiO_2 nanoparticles.

beamlines 13A1 and 17B3 of the National Synchrotron Radiation Research Center (NSRRC), Taiwan.

Fabrication and Characterization of Solar Cells. solar cells were fabricated with a device structure of ITO/PEDOT/PSS/polymer (0.3P3HT-0.7P2VP blend or cylindrical P3HT-*b*-P2VP)/TiO_2 nanoparticle (40 or 50 wt %)/TiO_2 nanorod hole blocking layer/Al. A solution of the 0.3P3HT-0.7P2VP blend (30 wt % of P3HT and 70 wt % of P2VP) was prepared in chlorobenzene according to the composition of the cylindrical copolymer. All concentrations of polymer solutions were 30 mg mL^{-1}. The TiO_2 solution was prepared with a concentration of 35 mg mL^{-1} in a cosolvent (pyridine/chloroform 2:1). The ITO-coated glass substrate was precleaned and treated with oxygen plasma prior to use. The polymer/TiO_2 NP layer was spin coated on the ITO at 1000 rpm from a mixed solution of polymer and nanoparticles. The layer was kept at about 100 nm. A 100 nm Al layer was deposited as the upper electrode under a vacuum of 5×10^{-6} Torr. The effective area of a single cell was 0.04 cm^2. The device was evaluated under simulated AM 1.5G irradiation (100 mW cm^{-2}) using a xenon lamp-based Newport 66902 150 W solar simulator at a power of 100 mW cm^{-2}. The $J-V$ characteristics of the device were measured using a Keithley 2410 electrometer.

Results and Discussion

Nicotinic Acid-Modified TiO_2 NPs. Nicotinic acid (NA)-modified TiO_2 NPs (NA-TiO_2 NPs) were characterized before being blended with polymers. Figure 1a is a schematic illustration of NA-TiO_2 NPs. The TiO_2 NPs were synthesized first by a sol−gel method,[25] followed by modification with NA. The NPs were characterized by TEM and FT-IR. Figure 1b shows ~3−5 nm NPs that are well separated without aggregation because NA is on the surface of TiO_2. Figure 1c shows that the characteristic IR absorption of NA (−C═O) 1700 cm^{-1} has been shifted to 1640 cm^{-1}, which indicates that the nicotinic acid has been chemically bonded to TiO_2 NPs.[27−29]

Morphologies of the P3HT-*b*-P2VP Copolymer/NA-TiO_2 NP Blend (Polymer-TiO_2 NP Hybrid). Figure 2 shows TEM images of how the TiO_2 NPs interact and are organized with the copolymer. The compatibility between NPs and polymers plays an important role in the final morphological structure of the blend. Because of the polar characteristic of TiO_2 NPs, they are expected to be placed near or in the domain of P2VP. Previous studies have shown that 40 wt % TiO_2 NPs are required to form continuous paths in the polymer−nanoparticle hybrid material in order to transport charge carriers in the solar cell.[30] Thus, we used this amount as the upper limit of TiO_2 NP loading in our study.

The hybrid of pure P3HT and TiO_2 NPs was also prepared for comparison. When pure P3HT was mixed with 40 wt % NA-TiO_2 NPs, a microscale phase separation occurred between the polar TiO_2 NPs and the hydrophobic P3HT (Figure 2a). Using 40 wt % NPs is too much to be accommodated in the nanodomain of self-assembled copolymers of P3HT-*b*-P2VP without disrupting their nanostructures except for the spherical copolymer.

The lamellar copolymer has a domain size of 15 nm. The morphology of the copolymer was still maintained when up to 10 wt % NPs was added (Figure 2b). When 10 wt % NPs was exceeded, the morphology was disrupted. However, the morphology of the cylindrical copolymer was still retained at >10 wt % NPs. Here, we used TEM to locate the TiO_2 NPs in the copolymer. The I_2-stained morphology (inset in Figure 2c; the dark domain is P2VP, and the white domain is P3HT) clearly indicates that the TiO_2 NPs are preferentially located within the P2VP domain of the copolymer as expected. When the amount of TiO_2 NPs increased to 20 wt %, the ordered cylindrical copolymer structure was preserved although at a larger domain size of 23 nm (Figure 2d). Disruption of the original cylindrical nanostructure occurs when loading the TiO_2 NPs to 40 wt % (Figure 2e). The I_2-stained nanodomain morphology (inset of Figure 2e) shows a disturbed morphology with twisting that is slightly enlarged by the high loading of TiO_2 NPs. The large domain size of the spherical copolymer (30 nm) can accommodate 40 wt % TiO_2 NPs without disrupting its morphology (Figure 2f). Thus, the effect of TiO_2 NPs concentration on the morphology of the cylindrical copolymer is more significant as compared to that of either lamellar or spherical copolymers. Hexagonal close packed (hcp) cylinder morphology is very desirable for high carrier transport in polymer solar cell application (i.e., a straight path between electrodes). Therefore, the effects of TiO_2 NP concentration on morphological, optical, and photovoltaic properties of cylindrical P3HT-*b*-P2VP are studied in detail, as follows.

SAXS Study of Polymer-TiO_2 NP Hybrids. Figure 3 shows the SAXS patterns of cylindrical P3HT-*b*-P2VP incorporated with different concentrations of TiO_2 NPs. The pure copolymer has a highly ordered HCP structure using a $1:4^{1/2}:7^{1/2}$ ratio of the wave vector q of visible peaks. As 10 wt % TiO_2 NPs are blended with copolymer, the feature peaks that correspond to the ordered HCP structure are still maintained. The observation of a maintained cylindrical structure is consistent with the TEM result (Figure 2c) at 10 wt % TiO_2 NPs. Additionally, SAXS also shows a slight downshift of the first peak (from 0.03661 to 0.03617 $Å^{-1}$), meaning that the domain size of the copolymer is enlarged by preferentially accommodating TiO_2 NPs within the P2VP domain. As the TiO_2 NPs concentration increases to 20 wt %, the feature peaks correlate to a highly ordered structure (peaks at $4^{1/2}$ and $7^{1/2}$ locations) that is still present but weaker as compared to those of the hybrid using 10 wt % NPs. However, the peaks of the ordered cylindrical structure disappear when a high concentration of NPs (40 wt %) is present. Only a broad first peak remains at this concentration. The disappearance of highly ordered structure peaks indicates that the original ordered structure was converted to

(27) Ivanda, M.; Musić, S.; Popović, S.; Gotić, M. *J. Mol. Struct.* **1999**, *480−481*, 645.
(28) Johnson, A. M.; Trakhtenberg, S.; Cannon, A. S.; Warner, J. C. *J. Phys. Chem. A* **2007**, *111*, 8139.
(29) Ekstrom, G. N.; McQuillan, A. J. *J. Phys. Chem. B* **1999**, *103*, 10562.
(30) Zeng, T. W.; Lin, Y. Y.; Chen, C. W.; Su, W. F.; Chen, C. H.; Liou, S. C.; Huang, H. Y. *Nanotechnology* **2006**, *17*, 5387.

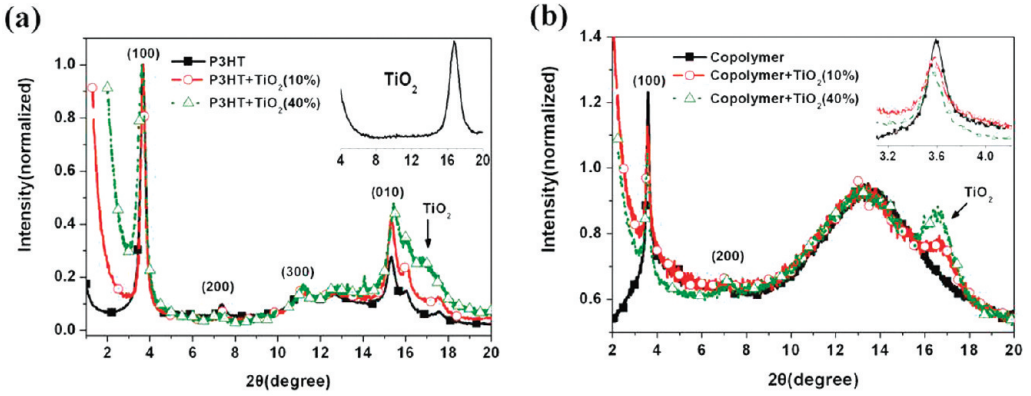

Figure 4. XRD patterns of (a) P3HT and (b) cylindrical P3HT-*b*-P2VP incorporating different amounts of TiO_2 NPs (0, 10, and 40 wt %).

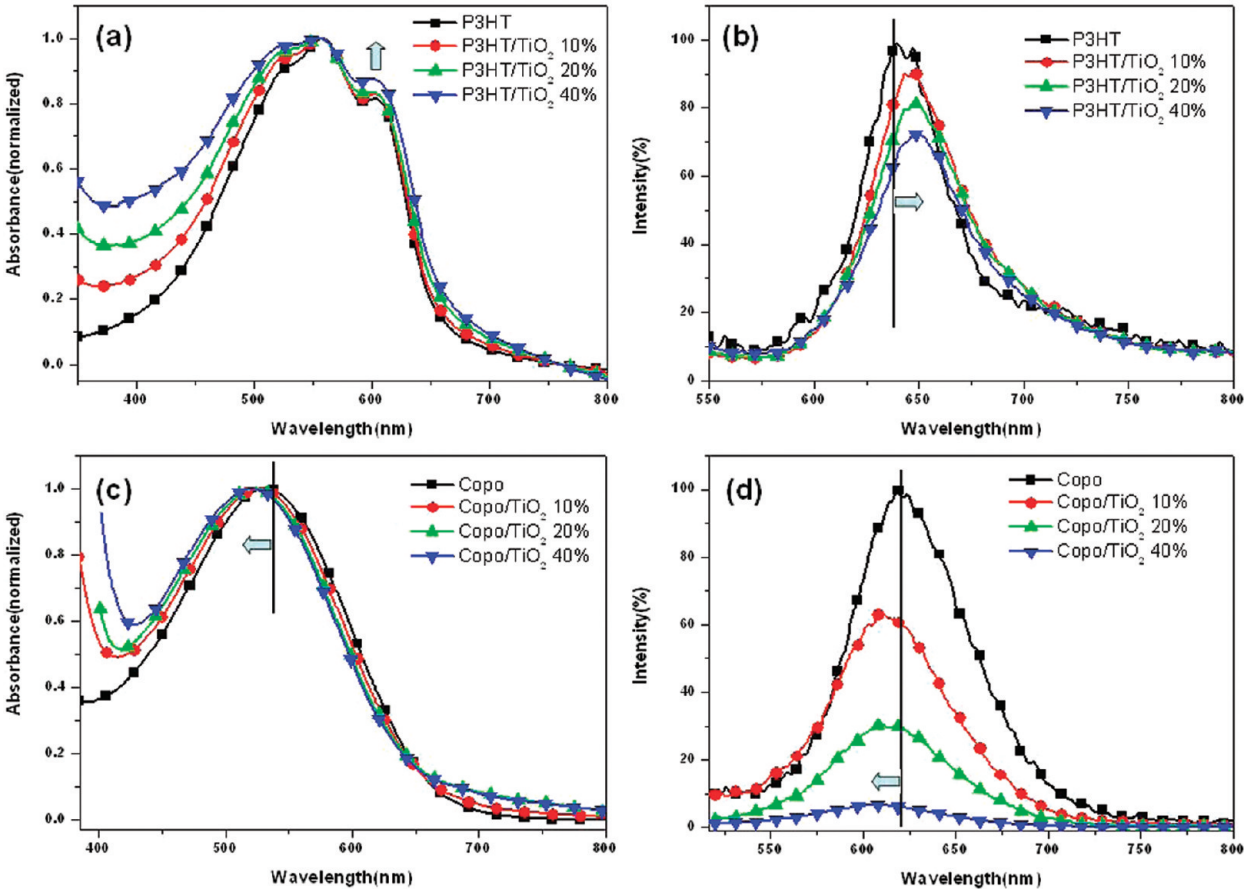

Figure 5. P3HT-TiO_2 hybrids with different amount of TiO_2 NPs: (a) absorption spectra and (b) PL spectra. Copolymer/TiO_2 hybrids with different amount of TiO_2 NPs: (c) absorption spectra and (d) PL spectra.

one with a random morphology. The result is consistent with the TEM observation (Figure 2e) at high TiO_2 NPs concentration. The first peak shifted to 0.03480 $Å^{-1}$ for the cylindrical copolymer containing 40 wt % TiO_2 NPs, and the domain size of the copolymer is 1.05 times that of the pristine copolymer.

XRD Study of Polymer-TiO_2 Hybrids. Figure 4 shows the XRD patterns of the hybrids containing different concentrations of TiO_2 NPs. For the P3HT-TiO_2 hybrid, the intensity of the (010) peak of P3HT (2θ at 15.3°) increases with increasing TiO_2 NP concentration (Figure 4a). This (010) peak is attributed to the intermolecular $\pi-\pi$ stacking of P3HT. The addition of TiO_2 NPs to P3HT facilitates $\pi-\pi$ stacking because of the aggregation of P3HT. Furthermore, the intensity of the peak referring to TiO_2 crystals (2θ at 16.7°) also increases with increasing concentration of TiO_2 NPs.

Figure 4b shows that the intensity of the (100) peak decreases (2θ at 3.4°) with increasing TiO_2 concentration in the cylindrical-copolymer-based hybrid. This (100) peak refers to the arrangement of inter-P3HT aligned by the alkyl side chain. Therefore, the observed decreasing intensity of the (100) peak is the result of a misalignment of the P3HT segment of the cylindrical copolymer. The segment is disrupted by the high loading of TiO_2 located within the P2VP domain. Such a disrupted P3HT alignment leads to the twisted morphology of copolymer as seen in the TEM study (Figure 2e).

Optical Properties of Polymer-TiO_2 Hybrids. In the hybrid of pure P3HT-TiO_2, both the normalized absorption and PL

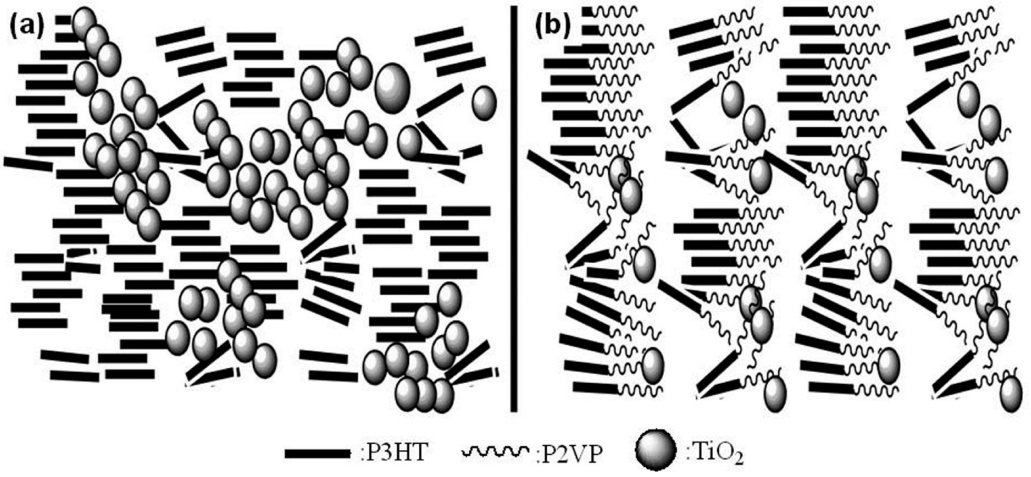

Figure 6. Schematic illustration of TiO_2 NPs interacting with polymers (a) P3HT, with microscale phase separation and aggregation, and (b) P3HT-*b*-P2VP, with P2VP domains accommodate TiO_2 NPs, which disturb the P3HT nanodomains with a twist.

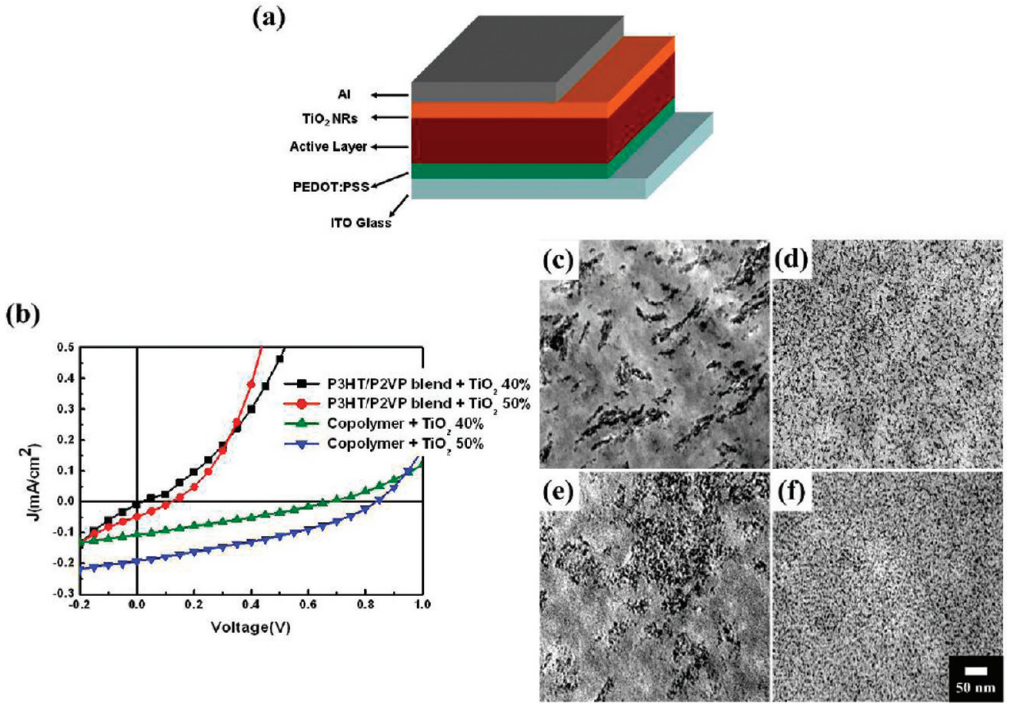

Figure 7. (a) Schematic illustration of a solar cell. (b) Current−voltage characteristics of polymers/TiO_2 solar cells under illumination (AM 1.5G, 100 mW cm^{-2}). TEM images of (c) a 0.3P3HT-0.7P2VP blend containing 40 wt % TiO_2, (d) cylindrical copolymer containing 40 wt % TiO_2, (e) a 0.3P3HT-0.7P2VP blend containing 50 wt % TiO_2, and (f) a cylindrical copolymer containing 50 wt % TiO_2.

(Figure 5a,b) spectra show a slight red shift of the main peaks with increasing concentration of TiO_2 NPs. The intensity of the shoulder peak (602 nm) in the absorption spectrum also increased with increasing TiO_2 NP concentration in the hybrid of pure P3HT-TiO_2. The shoulder peak at 602 nm is attributed to the intermolecular $\pi-\pi$ stacking structure of P3HT. Therefore, the optical spectra of P3HT/TiO_2 (UV−vis and PL) indicate that P3HT has a more highly ordered arrangement when blended with TiO_2 as compared with that in its pristine state.[31] The observation of a more highly ordered structure of P3HT from the optical properties is consistent with the XRD result (Figure 4a) that is due to the aggregation of P3HT in the blending system as discussed before (Figure 2a).

In contrast, P3HT-*b*-P2VP-TiO_2 shows a slight blue shift of the main peak in both absorption and PL spectra (Figure 5c,d) with increasing concentration of TiO_2 NPs. Pristine P3HT-*b*-P2VP molecules having longer P2VP chains with cylindrical or spherical structure exhibit a blue shift of the main peak and a decrease in the intensity of the shoulder peak (Figure S1) as compared to the pure P3HT or lamellar copolymer with a shorter P2VP chain. This means that the ordering of the P3HT domain of cylindrical copolymers has been disrupted by the longer P2VP chains. The ordering of the P3HT domain of the cylindrical copolymer is disrupted even further by increasing the TiO_2 NP loading. This decreases the effective conjugation length of P3HT, leading to a blue shift of the main peak in the optical spectra. These results are consistent with the XRD results discussed earlier (Figure 4b). It is interesting that the PL intensity of cylindrical P3HT-*b*-P2VP is

(31) Lin, Y. T.; Zeng, T. W.; Lai, W. Z.; Chen, C. W.; Lin, Y. Y.; Chang, Y. S.; Su, W. F. *Nanotechnology* **2006**, *17*, 5781.

Table 1. Properties of Polymer−Nanoparticle Hybrid Solar Cells

sample	V_{oc} (V)	J_{sc} (mA/cm^2)	FF (%)	PCE (%)
0.3P3HT-0.7P2VP blend (40% TiO_2)	0.018	0.009	22.51	0
0.3P3HT-0.7P2VP blend (50% TiO_2)	0.122	0.048	27.33	0.002
P3HT-*b*-P2VP (40% TiO_2)	0.674	0.106	28.57	0.020
P3HT-*b*-P2VP (50% TiO_2)	0.839	0.192	34.07	0.060

dramatically reduced when 40 wt % TiO_2 is used in the hybrid (Figure 5d). Compared with the hybrid of P3HT-TiO_2, the hybrid of P3HT-*b*-P2VP-TiO_2 exhibits no aggregation and thus there are many more interfaces allowing very effective exciton separation. Figure 6 schematically illustrates the effect of the addition of TiO_2 NPs on the morphologies of pure P3HT and cylindrical P3HT-*b*-P2VP copolymer. This well-ordered copolymer-NPs hybrid will facilitate the separation and transport of charge carriers for the BHJ solar cell application.

Photovoltaic Properties. For the purpose of comparison, two kinds of BHJ polymer solar cells were fabricated with a structure of ITO/PEDOT-PSS/active layer/hole blocking layer/Al as shown in Figure 7a. The difference between the solar cells is the composition of the active layer: cylindrical P3HT-*b*-P2VP/TiO_2 NPs and 0.3P3HT-0.7P2VP blend/TiO_2 NPs. The polymer blend of 30 wt % P3HT and 70 wt % P2VP (0.3P3HT-0.7P2VP blend) was selected to have a similar composition to cylindrical P3HT-*b*-P2VP that contains 25 wt % P3HT. The molecular weight of P3HT in the cells of P3HT-*b*-P2VP/TiO_2 NPs and 0.3P3HT-0.7P2VP blend/TiO_2 NPs was kept the same at about 7K Da. The TiO_2 nanorod layer was used as a hole-blocking layer according to our established device structure.[30,32−36] The efficiency of solar cells is evaluated by an AM 1.5 G solar simulator with an intensity of 100 mW/cm^2. The properties of solar cells tested include the open-circuit voltage (V_{oc}), short-circuit current (J_{sc}), fill factor (FF), and power conversion efficiency (η). The results are summarized in Table 1. Figure 7b shows the comparison of $I-V$ characteristics of the devices using copolymer and polymer blends. The cell fabricated from the 0.3P3HT-0.7P2VP blend/TiO_2 NP hybrid exhibits a power conversion efficiency (PCE) of close to 0% whereas that fabricated from cylindrical P3HT-*b*-P2VP/TiO_2 NPs has a PCE of 0.02% when both active layers contain 40 wt % TiO_2. The causes of such an extremely low PCE of the 0.3P3HT-0.7P2VP blend/TiO_2 NPs hybrid are twofold. First, the large extent of phase separation exhibited in the 0.3P3HT-0.7P2VP blend/TiO_2 NP hybrid results in an interface area that is too small to separate excitons effectively. Second, TiO_2 domains are isolated with interrupted paths that have difficulty transporting electrons (Figure 7c). In contrast, devices using cylindrical P3HT-*b*-P2VP/TiO_2 NPs showed a much higher efficiency than the 0.3P3HT-0.7P2VP blend/TiO_2 NPs because of their suitable morphology for effective charge separation and electron transport (Figure 7d). Furthermore, when we increased the TiO_2 content from 40 to 50 wt %, the PCE of 0.3P3HT-0.7P2VP blend/TiO_2 NPs increased from 0 to 0.002% and the PCE of cylindrical P3HT-*b*-P2VP/TiO_2 NPs increased from 0.020 to 0.060%. The increases in PCEs in both systems are due to the formation of a more continuous TiO_2 phase. The extent of the continuous phase is obviously smaller for the 0.3P3HT-0.7P2VP blend/TiO_2 NPs (Figure 7e) as compared to that of cylindrical P3HT-*b*-P2VP/TiO_2 NPs (Figure 7f), thus the copolymer PCE is 30 times higher. Moreover, the V_{oc} of this device is quite high at 0.839 when compared to that of most conventional polymer solar cell at 0.6, which is a desired property of high-efficiency solar cells and may originate from the blue shift of the copolymer (i.e., a higher HOMO). The efficiency of cylindrical copolymer-TiO_2 NP-based devices is not high because the hybrid material of this system contains a small amount of a light-harvesting component (i.e., 12.5 wt % from P3HT) and an insulating component of P2VP. The self-assembled conducting/conducting copolymer/nanoparticle system is currently under investigation with regard to high-efficiency BHJ solar cells. In summary, the hybrid materials prepared by simply blending P3HT-*b*-P2VPs with surface-modified TiO_2 NPs facilitate the formation of ordered and continuous domains.

Conclusions

The effects of TiO_2 nanoparticles on self-assembly behavior and optical and photovoltaic properties of the P3HT-*b*-P2VP block copolymer have been systematically studied. The TiO_2 nanoparticles (NA-TiO_2 NPs) were modified with nicotinic acid for ease of blending with polymers. The hybrid of pure P3HT and NA-TiO_2 NPs has aggregated morphology, strong $\pi-\pi$ stacking, and low-efficiency PL quenching due to the microscale phase separation between pure P3HT and NPs. In the hybrid of P3HT-*b*-P2VP and NA-TiO_2 NPs, the TiO_2 NPs are placed preferentially in the P2VP nanodomains of spherical, cylindrical, or lamellar copolymers. The ordering of nanostructures is dependent on the concentration of TiO_2 NPs and the type of P3HT-*b*-P2VPs. The small domain size (15 nm) of the lamellar copolymer is easily disturbed by the high loading of TiO_2 NPs. These TiO_2 NPs can be accommodated within the large domain size (30 nm) of spherical copolymers. The domain size of cylindrical copolymers is enlarged by 1.05 times after the incorporation of 40 wt % TiO_2 NPs. Excellent PL quenching behavior was observed in the cylindrical P3HT-*b*-P2VP/TiO_2 hybrid material. Our solar cells fabricated from self-assembled P3HT-*b*-P2VP/TiO_2 hybrid material exhibit more than a 30-fold improvement in power conversion efficiency as compared to that of 0.3P3HT-0.7P2VP blend/TiO_2 as a result of effective charge separation and transport obtained from the better suited morphology of the copolymer. These results pave the way for the further development of high-efficiency polymer−inorganic nanoparticle hybrid solar cells using self-assembled block copolymers.

Acknowledgment. We thank the National Science Council of Taiwan (NSC 95-3114-P-002-003-MY3, 98-3114-E-002-001, and 99-ET-E-002-001-ET) and the U.S. Air Force (AOARD-07-4014) for supporting this research. We also thank Mr. An-Jey Su of Duquesne University, Pittsburgh, PA, for editing the manuscript.

Supporting Information Available: UV−vis spectra of P3HT-*b*-P2VP with different morphologies and normalized absorption spectra of hybrids (P3HT/TiO_2 and cylindrical P3HT-*b*-P2VP/TiO_2) with the same thickness. This material is available free of charge via the Internet at http://pubs.acs.org.

(32) Chang, C. H.; Huang, T. K.; Lin, Y. T.; Lin, Y. Y.; Chen, C. W.; Chu, T. H.; Su, W. F. *J. Mater. Chem.* **2008**, *18*, 2201.
(33) Wu, M. C.; Chang, C. H.; Lo, H. H.; Lin, Y. S.; Chen, C. W.; Yen, W. C.; Lin, Y. Y.; Chen, Y. F.; Su, W. F. *J. Mater. Chem.* **2008**, *18*, 4097.
(34) Zeng, T. W.; Lo, H. H.; Chang, C. H.; Lin, Y. Y.; Chen, C. W.; Su, W. F. *Sol. Energy Mater. Sol. Cells* **2009**, *93*, 952.
(35) Lin, Y. Y.; Chu, T. H.; Li, S. S.; Chang, C. H.; Su, W. F.; Chang, C. P.; Chu, M. W.; Chen, C. W. *J. Am. Chem. Soc.* **2009**, *131*, 3644.
(36) Huang, Y. C.; Yen, W. C.; Liao, Y. C.; Yu, Y. C.; Hsu, C. C.; Ho, M. L.; Chou, P. T.; Su, W. F. *Appl. Phys. Lett.* **2010**, *96*, 123501.